

This article was downloaded by: [National Chiao Tung University 國立交通大學]

On: 24 April 2014, At: 18:42

Publisher: Taylor & Francis

Informa Ltd Registered in England and Wales Registered Number: 1072954 Registered office: Mortimer House, 37-41 Mortimer Street, London W1T 3JH, UK



Heat Transfer Engineering

Publication details, including instructions for authors and subscription information:

<http://www.tandfonline.com/loi/uhte20>

Heat Transfer and Flow Pattern Characteristics for HFE-7100 Within Microchannel Heat Sinks

Kai-Shing Yang^a, Yeau-Ren Jeng^b, Chun-Min Huang^b & Chi-Chuan Wang^c

^a Green Energy & Environment Laboratories, Industrial Technology Research Institute, Hsinchu, Taiwan

^b Department of Mechanical Engineering, National Chung Cheng University, Chia-Yi, Taiwan

^c Department of Mechanical Engineering, National Chiao Tung University, Hsinchu, Taiwan

Published online: 13 Oct 2011.

To cite this article: Kai-Shing Yang, Yeau-Ren Jeng, Chun-Min Huang & Chi-Chuan Wang (2011) Heat Transfer and Flow Pattern Characteristics for HFE-7100 Within Microchannel Heat Sinks, Heat Transfer Engineering, 32:7-8, 697-704, DOI: [10.1080/01457632.2010.509774](https://doi.org/10.1080/01457632.2010.509774)

To link to this article: <http://dx.doi.org/10.1080/01457632.2010.509774>

PLEASE SCROLL DOWN FOR ARTICLE

Taylor & Francis makes every effort to ensure the accuracy of all the information (the "Content") contained in the publications on our platform. However, Taylor & Francis, our agents, and our licensors make no representations or warranties whatsoever as to the accuracy, completeness, or suitability for any purpose of the Content. Any opinions and views expressed in this publication are the opinions and views of the authors, and are not the views of or endorsed by Taylor & Francis. The accuracy of the Content should not be relied upon and should be independently verified with primary sources of information. Taylor and Francis shall not be liable for any losses, actions, claims, proceedings, demands, costs, expenses, damages, and other liabilities whatsoever or howsoever caused arising directly or indirectly in connection with, in relation to or arising out of the use of the Content.

This article may be used for research, teaching, and private study purposes. Any substantial or systematic reproduction, redistribution, reselling, loan, sub-licensing, systematic supply, or distribution in any form to anyone is expressly forbidden. Terms & Conditions of access and use can be found at <http://www.tandfonline.com/page/terms-and-conditions>

Heat Transfer and Flow Pattern Characteristics for HFE-7100 Within Microchannel Heat Sinks

KAI-SHING YANG,¹ YEAU-REN JENG,² CHUN-MIN HUANG,²
and CHI-CHUAN WANG³

¹Green Energy & Environment Laboratories, Industrial Technology Research Institute, Hsinchu, Taiwan

²Department of Mechanical Engineering, National Chung Cheng University, Chia-Yi, Taiwan

³Department of Mechanical Engineering, National Chiao Tung University, Hsinchu, Taiwan

This study investigates the heat transfer characteristics and flow pattern for the dielectric fluid HFE-7100 within multiport microchannel heat sinks with hydraulic diameters of 480 μm and 790 μm . The test results indicate that the heat transfer coefficient for the smaller channel is generally higher than that of the larger channel. It is found that the heat transfer coefficients are roughly independent of heat flux and vapor quality for a modest mass flux ranging from 200 to 400 $\text{kg m}^{-2} \text{s}^{-1}$ at a channel size of 480 μm and there is a noticeable increase of heat transfer coefficient with heat flux for hydraulic diameters of 790 μm . The difference arises from flow pattern. However, for a smaller mass flux of 100 $\text{kg m}^{-2} \text{s}^{-1}$, the presence of flow reversal at an elevated heat flux for hydraulic diameters of 480 μm led to an appreciable drop of heat transfer coefficient. For a larger channel size of 790 μm , though the flow reversal is not observed at a larger heat flux, some local early partial dryout still occurs to offset the heat flux contribution and results in an unconceivable influence of heat flux. The measured heat transfer coefficients for hydraulic diameters of 790 μm are well predicted by the Cooper correlation. However, the Cooper correlation considerably underpredicts the test data by 35–85% for hydraulic diameters of 480 μm . The influence of mass flux on the heat transfer coefficient is quite small for both channels.

INTRODUCTION

Recently, microchannel heat sinks applicable to cooling of electronic chips and the microelectronic devices received intensive attention for their superior performance in handling higher flux demand. One of the simplest arrangements for the microchannel heat sinks takes the form of multiple parallel channels. There have been some detailed reviews concerning the two-phase heat transfer within microchannels [1–5]. One of the distinct features of the boiling heat transfer coefficient in a microchannel is that it usually remains unchanged with vapor quality in the low to medium quality region but reveals a considerable drop at a higher vapor quality region.

The authors are indebted to financial support from the Bureau of Energy of the Ministry of Economic Affairs, Taiwan. Also, a grant from National Science Council of Taiwan is appreciated.

Address correspondence to Professor Chi-Chuan Wang, Department of Mechanical Engineering, National Chiao Tung University, 1001 University Road, Hsinchu, Taiwan 300. E-mail: ccwang@mail.nctu.edu.tw

For practical applications of the liquid cooling to electronic equipment or integrated circuit (IC) components, dielectric fluid is often employed to avoid electric hazards. Because of the superior electrical and chemical properties, there have been a number of research studies concerning the heat transfer and fluid flow characteristics. However, results in connection with the dielectric fluids in microchannels were comparatively rare. A recent study by Chen and Garimella [6] presented the influence of dissolved air on the subcooled boiling performance with FC-77 fluid. Their investigation showed that degassing is very crucial in performing the heat transfer study of dielectric fluid. However, FC series coolants are Fluorinert liquids, which have high global warming potentials (GWP) and long atmospheric lifetimes. As such, a family of low-global-warming materials (HFE series, segregated hydrofluoroethers) designed to balance performance with favorable environmental and worker safety properties was then developed (3M [7]). In this regard, it is the purpose of this study to examine the associated heat transfer performance of HFE-7100 within multiport microchannel heat sinks, and flow visualization is also carried out to assist the understanding of measured heat transfer performance.

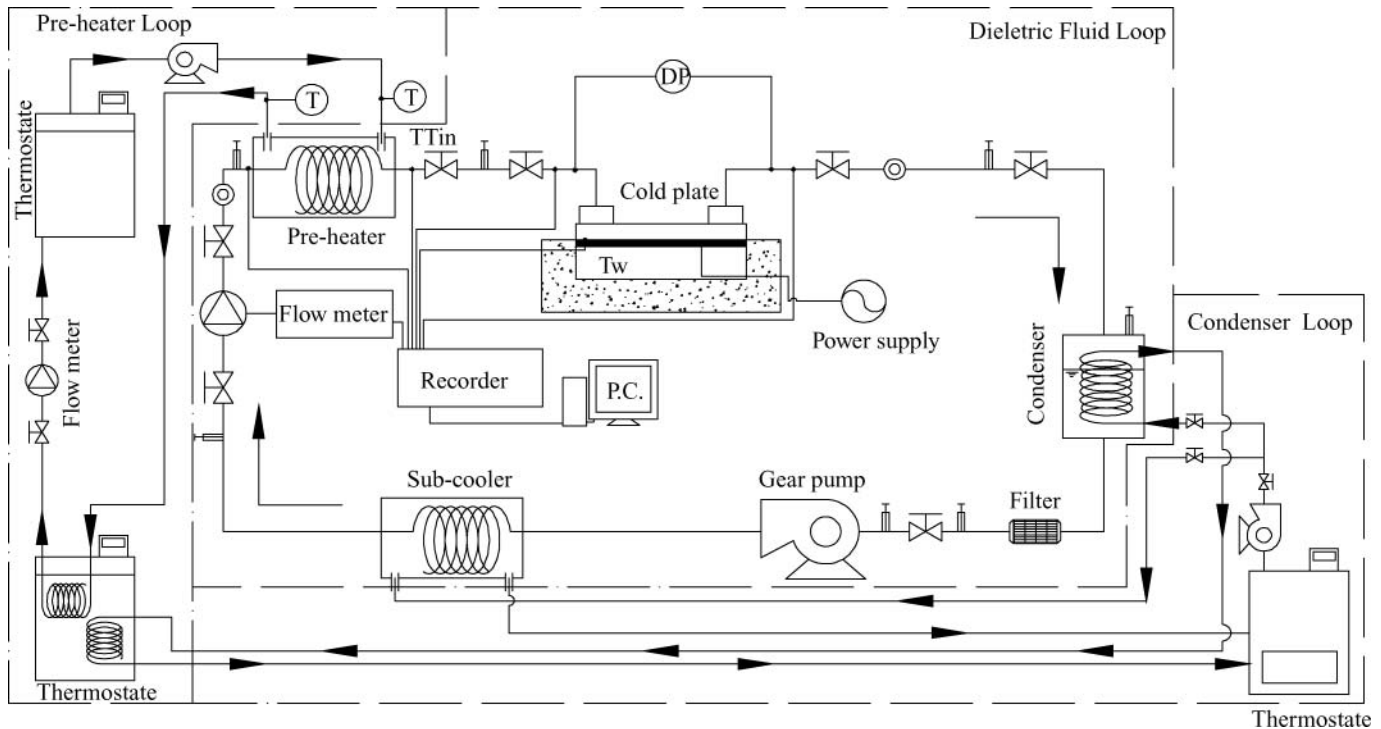


Figure 1 Schematic of the test loop.

EXPERIMENTAL SETUP

The schematic of the experimental apparatus and test section is shown in Figure 1. The experimental setup comprises the following as the main loop: a dielectric fluid loop, an HFE-7100 degassing device, a water loop for preheater, a subcooler, and a condenser, along with measurement units and data acquisition system. Among these loops, the preheater loop is for controlling the inlet quality into the test section whereas the subcooler loop is to ensure a fully liquid state before flowing into the preheater loop for easier calculation of the heat into the preheater.

Under ambient conditions, HFE7100 contains 53% of air by volume, implying that a unit of HFE-7100 liquid will contain 0.53 unit of air at standard pressure and temperature, which is equivalent to a concentration of about 366 ppm. For reference, the air content in water under similar condition is only 8.5 ppm. Hence, it is necessary to build up a degassing device for the test fluid. Figure 2 depicts the degassing device used in this study. As seen in Figure 2, the HFE-7100 is first circulated into a leak-free tank below which a uniform Kapton heater is placed. The HFE-7100 is then boiled up into vapor; it then carries along the non-condensable gas toward the Graham condenser, where the vapor HFE-7100 is condensed again and returns to the tank whereas the non-condensable material is relieved to the ambient. The degassing process continues for about 1 h to ensure that the deviation between the vapor pressure and its corresponding temperature of this measured vapor pressure is within $\pm 0.2^\circ\text{C}$.

The microchannel is made of copper via precise machining. The dimensions of the microchannel heat sinks are 25.4 mm

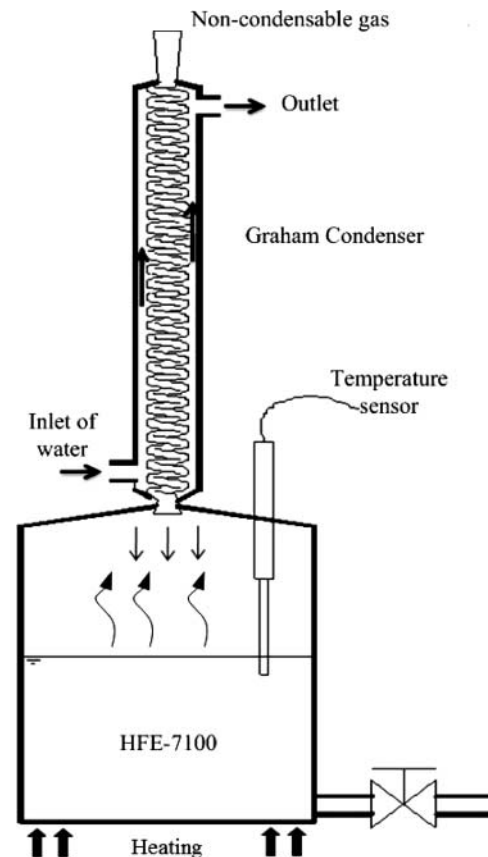


Figure 2 Degassing device of this study.

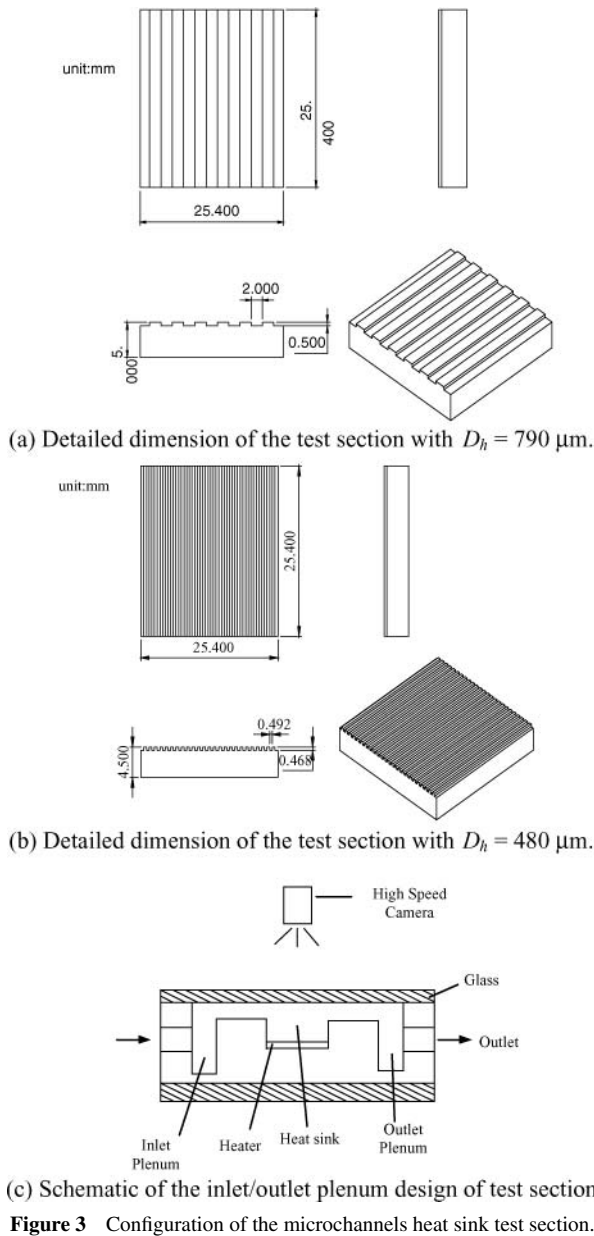


Figure 3 Configuration of the microchannels heat sink test section.

$\times 25.4 \text{ mm}$ with the corresponding rectangular microchannels with a hydrodynamic diameter of 480 and 790 μm , respectively. Its detailed dimensions along with the inlet location of the heat sink are shown in Figures 3a and b. Thermocouples are used to measure the surface and fluid temperature. A total of nine T-type thermocouples are placed beneath the cold plate for measurement of the average surface temperature, whereas two thermocouples are used to record the inlet and outlet temperatures of HFE-7100 across the cold plate. The thermocouples were precalibrated with an accuracy of 0.1°C . The test cold plate is located above a well-fitted Bakelite board. A transparent piece of glass is placed on top of the test section. Observations of flow patterns are obtained from images produced by a high-speed camera, type Redlake Motionscope PCI 8000s. The maximum camera shutter speed is $1/8000 \text{ s}$. The high-speed camera can be

placed at any position above the square microchannel. To minimize the effect of maldistribution caused by the inlet, an inlet plenum is made at the entrance of the test section whereas the inlet is placed at the bottom of the plenum, as seen in Figure 3c. With this design, the working fluid enters into the plenum and rises gradually before it distributes quite evenly into the multiport microchannels. Similarly, a downstream plenum having a similar configuration is exploited to reduce the effect from the downstream. A 10-mm-thick layer of rubber insulation is wrapped around the cold plate and Bakelite board to minimize the heat loss to the surrounding. At the inlet and outlet of the cold plate, a precise differential pressure transducer having an accuracy of 0.1% is used to measure the pressure drop across the cold plate.

DATA REDUCTION

The measured temperatures at the nine locations underneath the microchannels were first corrected to obtain the corresponding wall temperature at the inner wall surface via a one-dimensional conduction equation, i.e.,

$$\bar{T}_{wall} = \bar{T}_{b,wall} - \frac{Q'\delta_w}{k_s A} \quad (1)$$

where \bar{T}_{wall} is the average surface temperature of cold plate whereas $\bar{T}_{b,wall}$ is the average surface temperature beneath the cold plate and δ_w is the thickness of the cold plate; k_s is the corresponding thermal conductivity of cold plate (copper); and Q' is the heat transfer into the cold plate, and is obtained by subtracting the heat loss from the input power:

$$Q' = Q_{input} - Q_{loss} \quad (2)$$

where Q_{input} ($I \times V$) is the supplied input power and Q_{loss} is the heat lost across the Bakelite segment, which can be estimated from the one-dimensional heat conduction equation from the measured temperature difference of the thermocouples that were placed above and below the Bakelite segment. The average heat transfer coefficient can be obtained as follows:

$$h = \frac{Q'}{A\Delta T_m} \quad (3)$$

where A is total surface area and ΔT_m is the effective mean temperature difference, and is calculated from the following:

$$\Delta T_m = \bar{T}_{wall} - T_s \quad (4)$$

During the two-phase experiment, the inlet vapor quality is controlled by a double-pipe heat exchanger that is circulated with controlled water temperature by a thermostat. Note that the HFE-7100 is initially subcooled before entering the preheater. Hence the corresponding thermodynamic quality can be estimated from the simple energy balance from the preheater:

$$x_{in} = \frac{Q_{water} - \dot{m}c_{p,HFE7100}\Delta T_{sub}}{\dot{m}i_{fg}} \quad (5)$$

Notice that ΔT_{sub} is the inlet subcooling of HFE7100, and l_{fg} the latent heat of HFE-7100. The test conditions within the test sample are all at saturated state.

RESULTS AND DISCUSSION

Figure 4 presents the two-phase convective heat transfer coefficient versus vapor quality subject to the influence of heat flux for the two test microchannels ($D_h = 480$ and $790 \mu\text{m}$) with $G = 100, 200,$ and $400 \text{ kg m}^{-2} \text{ s}^{-1}$. The saturation pressure is fixed at 110 kPa before entering the test section and the prescribed heat flux is 25 kW m^{-2} or 37.5 kW m^{-2} , respectively. Normally the heat transfer coefficients for $D_h = 480 \mu\text{m}$ exceed those of $D_h = 790 \mu\text{m}$. The results are in line with recent studies [8, 9]). On the other hand, for a moderate mass flux of 200 and $400 \text{ kg m}^{-2} \text{ s}^{-1}$, the heat transfer coefficients are relatively invariant with the heat flux and vapor quality, whereas a noticeable influence of heat flux on the heat transfer coefficient is encountered for $D_h = 790 \mu\text{m}$, but it still holds comparatively unchanged with respect to mass flux and vapor quality. Upon the influence of heat flux, the two distinct trends for the two test channels imply different mechanisms behind them. The appreciable influence of heat flux on the heat transfer coefficient for $D_h = 790 \mu\text{m}$ implies that the nucleate boiling plays an essential role. By contrast, for a smaller hydraulic diameter of $480 \mu\text{m}$, a confinement effect takes control and the generated bubbles easily occupying the channel engender early establishment of a churn/annular flow pattern. In this regard, bubble nucleation is not the sole heat transfer mechanism, and the thin film evaporation for the annular flow and the microlayer evaporation between elongated bubble and wall also contribute to the heat transfer. As a consequence, one can see a rather small influence of heat flux on the heat transfer performance for $D_h = 480 \mu\text{m}$, whereas a detectable influence of heat flux is seen for $D_h = 790 \mu\text{m}$. For a better interpretation of the aforementioned argument, a typical progress of flow pattern with $G = 400 \text{ kg m}^{-2} \text{ s}^{-1}$ subject to the influence of heat flux and channel size is shown in Table 1. For the smaller size channel ($D_h = 480 \mu\text{m}$), the dominant flow pattern, except that for $x = 0.12$ and $q = 25 \text{ kW m}^{-2}$, is almost annular throughout the test range. Conversely, the flow pattern develops from elongated bubble, to slug, to churn, and finally into annular flow for $D_h = 790 \mu\text{m}$ as the vapor quality is increased. Thus, the smaller channel reveals a rather small influence of heat flux, while the latter one is prone to being influenced by heat flux. A sharp decline of the heat transfer coefficient is seen for $G = 200 \text{ kg m}^{-2} \text{ s}^{-1}$ at $q = 37.5 \text{ kW m}^{-2}$ and $x > 0.7$. This is apparently due to the early dryout of working fluid within the microchannel.

However, for a smaller mass flux like $G = 100 \text{ kg m}^{-2} \text{ s}^{-1}$, the heat transfer coefficients for both channels reveal a quite different characteristic than those for larger mass flux. Despite the heat transfer coefficient for the smaller channel still exceeding that of the larger channel, the larger channel does not reveal an apparent dependence of heat flux, while the smaller channel with $q = 37.5 \text{ kW m}^{-2}$ shows an appreciable decline

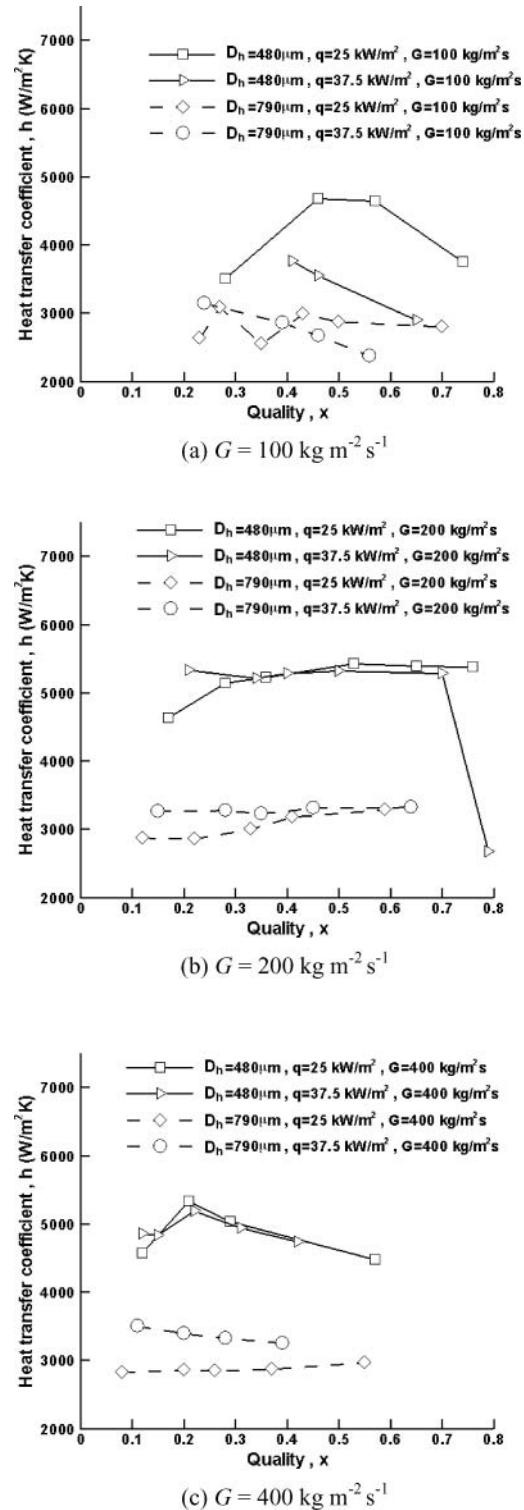
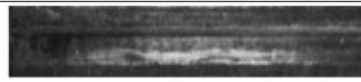
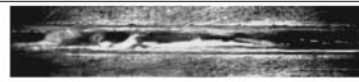







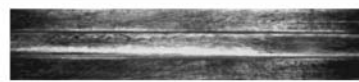


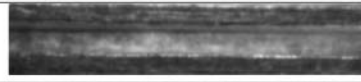

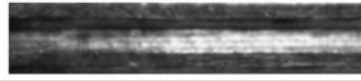





Figure 4 Two-phase heat transfer coefficient versus vapor quality subject to influence of heat flux for $G = 100, 200,$ and $400 \text{ kg m}^{-2} \text{ s}^{-1}$.

with the rise of vapor quality. A close examination of the flow visualizations indicates that it is also related to the flow pattern. In fact, the decline of heat transfer coefficient for $D_h = 480 \mu\text{m}$ at $G = 100 \text{ kg m}^{-2} \text{ s}^{-1}$ with $q = 37.5 \text{ kW m}^{-2}$ is caused by the

Table 1 Flow pattern for both test channels with $G = 400 \text{ kg m}^{-2} \text{ s}^{-1}$

		Flow direction →	
x	q kWm^{-2}	$D_h = 480 \mu\text{m}$	$D_h = 790 \mu\text{m}$
0.12	25		
	37.5		
0.21	25		
	37.5		
0.29	25		
	37.5		
0.40	25		
	37.5		
0.57	25		

presence of flow reversal in some part of the multiport channels. The flow reversal is found to be strongly related to the applied heat flux and is especially pronounced when the mass flux is low. Some typical photos showing the progress of vapor slug within the microchannel for $G = 100 \text{ kg m}^{-2} \text{ s}^{-1}$, $D_h = 480 \mu\text{m}$, are seen in Table 2a. As depicted in the photos, for a higher heat flux of 37.5 kW m^{-2} , one can find that within some channels the vapor slug is moving backward, yet it expands with time due to heat addition. Conversely, for a lower heat flux of 25 kW/m^2 , the vapor slug moved with the main flow direction regardless of the vapor slug still expanding along the flow direction.

Wang et al. [10] found that at a given heat flux and inlet water temperature, depending on the mass flux, stable and unstable flow boiling regimes existed. For a $186\text{-}\mu\text{m}$ microchannel, they identified that the stable/unstable flow regime is related to the ratio of q/G . Unstable flow boiling persists when $q/G > 0.96 \text{ kJ/kg}$. Though the present oscillation flow conditions do not quantitatively agree with the q/G ratio reported by Wang et al. [10], they are quite similar to the Wang et al. results to some extent. The flow oscillation is quite complex, for it resorts to the difference in working fluid, operating conditions, and channel size. Generally, a larger value of q/G will be prone to oscillation.

On the other hand, the flow reversal phenomenon is not seen for $D_h = 790 \mu\text{m}$ at $q = 37.5 \text{ kW m}^{-2}$ and $G = 100 \text{ kg m}^{-2} \text{ s}^{-1}$

as shown in Table 2b. Therefore, one can see that there is no apparent decline of heat transfer coefficient when $x < 0.5$. However, a larger heat flux still may bring about local early partial dryout within the microchannel, leading to some deteriorations of heat transfer performance; the effect offsets the influence of heat flux and results in an insignificant variation of the heat transfer coefficients for $D_h = 790 \mu\text{m}$ at $G = 100 \text{ kg m}^{-2} \text{ s}^{-1}$.

The flow reversal within some microchannels implies that some other channels must have a much higher mass flux, for the average mass flux is fixed during the experiments. Note that the origin of the flow reversal is due to the expansion of vapor slug during heat addition. With a higher heat input, the onset of forming vapor slugs is rather violent and it can easily fill up the channel. The resultant phenomenon pushes the liquid at the tail of the expanding slug, and this acts like a roadblock to the main flow within the microchannel. As a consequence, flow reversals occur in some of the channels. An analogous phenomenon was also reported by Kandlikar et al. [11]. This phenomenon becomes even more severe when the heat flux is further raised, thereby leading to an appreciable decline of heat transfer coefficient versus vapor quality.

Figure 5 depicts the two-phase convective heat transfer coefficient versus vapor quality subject to the influence of mass flux for the two test microchannels ($D_h = 480$ and $790 \mu\text{m}$)

Table 2a Progress of the flow pattern with $G = 100 \text{ kg m}^{-2} \text{ s}^{-1}$ and $x_{ave} = 0.4$ for $D_h = 480 \mu\text{m}$

Time (s)	Flow Reversal, $q = 37.5 \text{ kW m}^{-2}$ →
$t = 0.002$	
$t = 0.004$	
$t = 0.006$	
$t = 0.008$	
$t = 0.012$	
	Normal, $q = 25 \text{ kW/m}^2$ →
$t = 0.002$	
$t = 0.004$	
$t = 0.006$	
$t = 0.008$	
$t = 0.012$	

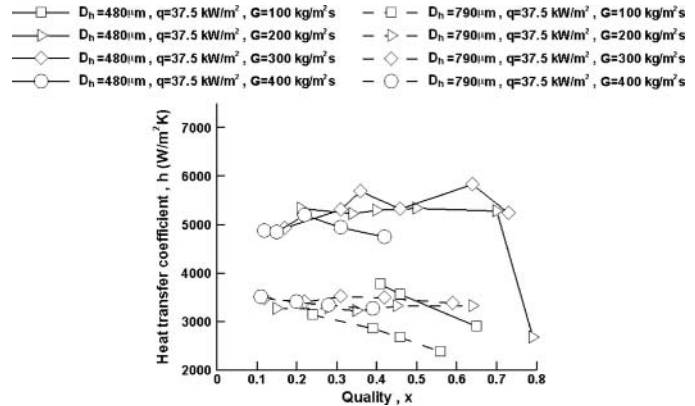


Figure 5 Effect of mass flux on the two-phase heat transfer coefficient.

generally slightly lower than that of $G = 300 \text{ kg m}^{-2} \text{ s}^{-1}$. It is not totally clear about this phenomenon but it is likely that the decrease in heat transfer coefficient may be associated with the suppression of nucleate boiling caused by the contribution of forced convection. The measured heat transfer coefficients are compared with the Cooper correlation [12]. The correlation is given as

$$h_C = 55q^{0.67} M^{-0.5} P_r^m (-\log_{10} P_r)^{-0.55} \quad (6)$$

$$m = 0.12 - 0.2 \log_{10} R_p \quad (7)$$

As reported by Stephan and Abdelsalam [13], the commercial-finish copper tubes generally have a surface roughness of $0.4 \mu\text{m}$. Therefore, the surface roughness, R_p , is given as $0.4 \mu\text{m}$ in the present calculation.

The overall deviation amid the predicted values versus the measurements for $D_h = 790 \mu\text{m}$ is within $\pm 30\%$. On the other hand, for $D_h = 480 \mu\text{m}$, the Cooper correlation is found to considerably underpredict the measurements, ranging from 35% to approximately 85%. Notice that the Cooper correlation was originally developed for nucleate boiling and did not contain the effect of mass flux. The good agreement between Cooper correlation and the measurements for $D_h = 790 \mu\text{m}$ implies a dominance of nucleate boiling. Results of the comparisons confirm with the discussions already drawn from the discussion of Figure 4. The results are also analogous to those reported by Bertsch et al. [14], who performed a comparative analysis of heat transfer coefficients against various correlations. They had compiled 1847 measurements from 10 independent sources with hydraulic diameter ranging from 0.16 mm to 2.01 mm, and performed comparisons with the database against 12 correlations. Their comparisons indicated that the Cooper correlation gives the best overall predictive ability. However, it should be mentioned that for a smaller size like $D_h = 480 \mu\text{m}$, the Cooper correlation considerably underpredicts the present test data due to a significant change of flow pattern. This trend is also reported by Harirchian and Garimella [9].

with $G = 100, 200, 300,$ and $400 \text{ kg m}^{-2} \text{ s}^{-1}$. The saturation pressure is also fixed at 110 kPa, having a prescribed heat flux of 37.5 kW m^{-2} . As illustrated in the figure, except for $G = 100 \text{ kg m}^{-2} \text{ s}^{-1}$ where flow reversal may occur, the effect of mass flux on the heat transfer coefficient is not as evident as that of heat flux. This is applicable for both test channels. In the meantime, for $D_h = 480 \mu\text{m}$, despite the fact that there is no significant difference upon the measured heat transfer coefficients subject to mass flux variation, it is interesting to know that the heat transfer coefficients for $G = 400 \text{ kg m}^{-2} \text{ s}^{-1}$ are

Table 2b Progress of the flow pattern with $G = 100 \text{ kg m}^{-2} \text{ s}^{-1}$ and $x_{ave} = 0.4$ for $D_h = 790 \mu\text{m}$

Time (s)	No Flow Reversal, $q = 37.5 \text{ kW m}^{-2}$ →
$t = 0.002$	
$t = 0.012$	

CONCLUSIONS

This study examines the heat transfer characteristics of the dielectric fluid HFE-7100 within multiport microchannel heat sinks having hydraulic diameters of 480 μm and 790 μm , respectively. Flow visualization is also conducted in this study. For the same heat flux and mass flux, the test results indicate that the heat transfer coefficient for the smaller channel is generally higher than that of the larger channel. Depending on the channel size, the test results show that the heat transfer coefficients are roughly independent of heat flux and vapor quality for a modest mass flux ranging from 200 to 400 $\text{kg m}^{-2} \text{s}^{-1}$ for a channel size of 480 μm . Conversely, a noticeable increase of heat transfer coefficient with heat flux for $D_h = 790 \mu\text{m}$ is observed. The corresponding flow visualization confirms that the difference arises from flow pattern. The major flow pattern for the smaller channel is dominated by churn/annular flow, leading to a negligible influence of heat flux, yet for a larger channel the flow pattern develops from bubbly, to elongated bubble, slug, and churn/annular, which brings about a detectable influence of heat flux. However, for a smaller mass flux of 100 $\text{kg m}^{-2} \text{s}^{-1}$, the presence of flow reversal at an elevated heat flux for $D_h = 480 \mu\text{m}$ is seen, leading to an appreciable drop of heat transfer coefficient. For a larger channel size of 790 μm , though the flow reversal is not observed at a larger heat flux, some local early partial dryout still occurs to offset the heat flux contribution, and results in an unconceivable influence of heat flux. The measured heat transfer coefficients for $D_h = 790 \mu\text{m}$ are well predicted by the Cooper correlation. However, the Cooper correlation considerably underpredicts the test data by 35–85% for $D_h = 480 \mu\text{m}$. For the same heat flux, the influence of mass flux on the heat transfer coefficient is quite small, and this is applicable for both microchannels ($D_h = 480 \mu\text{m}$ and 790 μm).

NOMENCLATURE

A	surface area (m^2)
c_p	specific heat ($\text{J kg}^{-1} \text{K}^{-1}$)
D_h	hydraulic diameter (m)
G	mass flux ($\text{kg m}^{-2} \text{s}^{-1}$)
h	heat transfer coefficient ($\text{W m}^{-2} \text{K}^{-1}$)
h_C	boiling heat transfer coefficient for Cooper correlation ($\text{W m}^{-2} \text{K}^{-1}$)
I	current (A)
i_{fg}	latent heat of HFE-7100 (J kg^{-1})
k_s	thermal conductivity of cold plate ($\text{W m}^{-1} \text{K}^{-1}$)
m	molecular weight (kg/kmol)
\dot{m}	mass flow rate (kg s^{-1})
P_r	reduced pressure
q	heat flux (W m^{-2})
Q'	heat transfer into the cold plate (W)
Q_{input}	supplied input power (W)
Q_{loss}	heat loss across backlite (W)
R_p	surface roughness (μm)

t	time (s)
T_s	saturation temperature (K)
\bar{T}_{wall}	average surface temperature of cold plate (K)
$\bar{T}_{b,wall}$	average surface temperature beneath the cold plate (K)
V	voltage (V)
x	vapor quality
x_{ave}	average vapor quality of inlet and outlet

Greek Symbols

δ_w	thickness of the cold plate (m)
ΔT_m	effective mean temperature difference (K)
ΔT_{sub}	inlet subcooling of HFE-7100 (K)

REFERENCES

- [1] Thome, J. R., Boiling in Microchannels: A Review of Experiment and Theory, *International Journal of Heat and Fluid Flow*, vol. 25, pp. 128–139, 2004.
- [2] Kandlikar, S., Garimella, S., Li, D., Colin, S., and King, M. R., *Heat Transfer and Fluid Flow in Minichannels and Microchannels*, Elsevier Science, Oxford, UK, 2006.
- [3] Ribatski, G., Wojtan, L., and Thome, J. R., An Analysis of Experimental Data and Prediction Methods for Two-Phase Frictional Pressure Drop and Flow Boiling Heat Transfer in Micro-Scale Channels, *Experimental Thermal & Fluid Science*, vol. 31, pp. 1–19, 2006.
- [4] Thome, J., State-of-the-Art Overview of Boiling and Two-Phase Flows in Microchannels, *Heat Transfer Engineering*, vol. 27, pp. 4–19, 2006.
- [5] Cheng, P., Wu, H. Y., and Hong, F. J., Phase-Change Heat Transfer in Microsystems, *Journal of Heat Transfer*, vol. 129, pp. 101–107, 2007.
- [6] Chen, T., and Garimella, S. V., Effects of Dissolved Air on Subcooled Flow Boiling of a Dielectric Coolant in a Microchannel Heat Sink, *ASME Journal of Electronic Packaging*, vol. 128, pp. 398–404, 2006.
- [7] 3M, *Thermal Management Fluids and Services*, 3M, St. Paul, MN, 2003.
- [8] Qi, S. L., Zhang, P., Wang, R. Z., and Xu, L. X., Flow Boiling of Liquid in Micro-Tubes: Part II—Heat Transfer Characteristics and Critical Heat Flux, *International Journal of Heat and Mass Transfer*, vol. 50, pp. 5017–5030, 2007.
- [9] Harirchian, T., and Garimella, S. V., The Critical Role for Channel Cross-Sectional Area in Microchannel Flow Boiling Heat Transfer, *International Journal of Multiphase Flow*, vol. 35, pp. 349–362, 2009.
- [10] Wang, G., Cheng, P., and Wu, H., Unstable and Stable Flow Boiling in Parallel Microchannels and in a Single Microchannel, *International Journal of Heat and Mass Transfer*, vol. 50, pp. 4297–4310, 2007.

- [11] Kandlikar, S. G., Kuan, W. K., Willistein, D. A., and Borrelli, J., Stabilization of Flow Boiling in Microchannels Using Pressure Drop Elements and Fabricated Nucleation Sites, *Journal of Heat Transfer*, vol. 39, pp. 159–167, 2006.
- [12] Cooper, M. G., Heat Flow Rates in Saturated Nucleate Pool Boiling—A Wide-Ranging Examination Using Reduced Properties, *Advances in Heat Transfer*, vol. 16, pp. 157–239, 1984.
- [13] Stephan, K., and Abdelsalam, M., Heat Transfer Correlations for Natural Convection Boiling, *International Journal of Heat and Mass Transfer*, vol. 23, pp. 73–87, 1980.
- [14] Bertsch, S. S., Groll, E. A., and Garimella, S. V., Review and Comparative Analysis of Studies on Saturated Flow Boiling in Small Channels, *Nanoscale and Microscale Thermophysical Engineering*, vol. 12, pp. 187–227, 2008.



Yeau-Ren Jeng is a professor in the Department of Mechanical Engineering, National Chung Cheng University, Taiwan. He received his Ph.D. from the Department of Mechanical Engineering, Case Western Reserve University, Cleveland, OH. His research areas include tribology, nanomechanics, nanotechnology, surface texture, electrical packaging, and semiconductor fabrication.



Chun-Min Huang is a master's degree student in the Department of Mechanical Engineering, National Chung Cheng University, Taiwan. His current research is in the microscale heat transfer technology.



Chi-Chuan Wang is a professor in the Department of Mechanical Engineering, National Chiao Tung University, Hsinchu, Taiwan. He received his B.S., M.S., and Ph.D. from the Department of Mechanical Engineering of National Chiao-Tung University, Hsinchu, Taiwan, during 1978–1989. He then joined the Energy & Environment Research Lab., Industrial Technology Research Institute, Hsinchu, for about 20 years (1989–2009), conducting research related to enhanced heat transfer, multiphase systems, micro-

scale heat transfer, membrane separation, and heat pump technology. He is also a regional editor of the *Journal of Enhanced Heat Transfer* and an associate editor of *Heat Transfer Engineering*.



Kai-Shing Yang is a scientific researcher at the Green Energy & Environment Research Laboratories, ITRI, Taiwan. He received his M.S. and Ph.D. in mechanical engineering from National Yunlin University of Science and Technology, Taiwan, during 1998–2004 and joined the Energy & Environment Research Lab., Industrial Technology Research Institute, Hsinchu, Taiwan, during 2004–2009. His research areas include enhanced heat transfer and multiphase system technology.